Cellular/Molecular

$Ca_v1.4\alpha1$ Subunits Can Form Slowly Inactivating Dihydropyridine-Sensitive L-Type Ca^{2+} Channels Lacking Ca^{2+}-Dependent Inactivation

Alexandra Koschak,[1] Daniel Reimer,[1,2] Doris Walter,[1] Jean-Charles Hoda,[1] Thomas Heinzle,[2] Manfred Grabner,[2] and Jörg Striessnig[1]

[1]Institut für Pharmazie, Abteilung Pharmakologie und Toxikologie, A-6020 Innsbruck, Austria, [2]Institut für Biochemische Pharmakologie, A-6020 Innsbruck, Austria

The neuronal L-type calcium channels (LTCCs) $Ca_v1.2\alpha1$ and $Ca_v1.3\alpha1$ are functionally distinct. $Ca_v1.3\alpha1$ activates at lower voltages and inactivates more slowly than $Ca_v1.2\alpha1$, making it suitable to support sustained L-type Ca^{2+} inward currents ($I_{Ca,L}$) and serve in pacemaker functions. We compared the biophysical and pharmacological properties of human retinal $Ca_v1.4\alpha1$ using the whole-cell patch-clamp technique after heterologous expression in tsA-201 cells with other L-type $\alpha1$ subunits. $Ca_v1.4\alpha1$-mediated inward Ba^{2+} currents (I_{Ba}) required the coexpression of $\alpha2\delta1$ and $\beta3$ or $\beta2a$ subunits and were detected in a lower proportion of transfected cells than $Ca_v1.3\alpha1$. I_{Ba} activated at more negative voltages (5% activation threshold; −39mV; 15 mM Ba^{2+}) than $Ca_v1.2\alpha1$ and slightly more positive than $Ca_v1.3\alpha1$. Voltage-dependent inactivation of I_{Ba} was slower than for $Ca_v1.2\alpha1$ and $Ca_v1.3\alpha1$ (~50% inactivation after 5 sec; $\alpha2\delta1 + \beta3$ coexpression). Inactivation was not increased with Ca^{2+} as the charge carrier, indicating the absence of Ca^{2+}-dependent inactivation. $Ca_v1.4\alpha1$ exhibited voltage-dependent, G-protein-independent facilitation by strong depolarizing pulses. The dihydropyridine (DHP)-antagonist isradipine blocked $Ca_v1.4\alpha1$ with ~15-fold lower sensitivity than $Ca_v1.2\alpha1$ and in a voltage-dependent manner. Strong stimulation by the DHP BayK 8644 was found despite the substitution of an otherwise L-type channel-specific tyrosine residue in position 1414 (repeat IVS6) by a phenylalanine. $Ca_v1.4\alpha1 + \alpha2\delta1 + \beta$ channel complexes can form LTCCs with intermediate DHP antagonist sensitivity lacking Ca^{2+}-dependent inactivation. Their biophysical properties should enable them to contribute to sustained $I_{Ca,L}$ at negative potentials, such as required for tonic neurotransmitter release in sensory cells and plateau potentials in spiking neurons.

Key words: **calcium channels; calcium-dependent inactivation; retina; calcium channel blockers; dihydropyridines; congenital stationary night blindness**

Introduction

Many cellular functions are controlled by a depolarization-induced influx of Ca^{2+} ions from the extracellular space through voltage-gated Ca^{2+} channels. In neurons, Ca^{2+} influx through presynaptic N-, P/Q-, and, to a limited extent, R-type Ca^{2+} channels is tightly coupled to neurotransmitter release from nerve terminals (stimulus-secretion coupling) (Catterall, 2000). L-type Ca^{2+} channels (LTCCs) are primarily targeted to dendrites and the cell soma (Catterall, 2000) and are responsible for Ca^{2+} signals, which activate signaling pathways controlling gene transcription (Graef et al., 1999).

We (Koschak et al., 2001), and others (for review, see Lipscombe, 2002), have recently found that $Ca_v1.2\alpha1$ and $Ca_v1.3\alpha1$ LTCCs possess distinct functional properties that thus allow them to serve distinct neuronal functions. $Ca_v1.3\alpha1$ channels activate at more negative voltages, inactivate slower during depolarizing pulses, and exhibit lower dihydropyridine (DHP) antagonist sensitivity than $Ca_v1.2\alpha1$. Their biophysical properties make them highly suitable to mediate tonic neurotransmitter release in sensory cells (such as in cochlear inner hair cells) (Platzer et al., 2000) to support plateau potentials in spiking neurons (Carlin et al., 2000; Alaburda et al., 2002; Morisset and Nagy, 2000) and contribute to diastolic depolarization and pacemaking in the sinoatrial node (Mangoni et al., 2003) (for review, see Lipscombe, 2002). In the mammalian retina, $Ca_v1.3\alpha1$ subunits are expressed in photoreceptor nerve terminals and selected bipolar cell synapses (Morgans et al., 1998; Taylor and Morgans, 1998; Morgans, 1999). $I_{Ca,L}$ in photoreceptors and bipolar cells shares most features of heterologously expressed $Ca_v1.3\alpha1$ currents. It was therefore proposed that this channel underlies retinal $I_{Ca,L}$ (Wilkinson and Barnes, 1996).

Recently, $Ca_v1.4\alpha1$ subunits were discovered as a putative neuronal LTCC subunit (Bech-Hansen et al., 1998; Strom et al., 1998). $Ca_v1.4\alpha1$ is expressed predominantly in the retina but also in other neurons such as dorsal root ganglia (Murakami et al., 2001). In the mammalian retina, its expression pattern resembles $Ca_v1.3\alpha1$. $Ca_v1.4\alpha1$ immunoreactivity has also been localized in

Received Jan. 21, 2003; revised April 16, 2003; accepted April 24, 2003.

This work was supported by Austrian Science Fund Grants P-14541 and P-14820 (J.S.), the Österreichische National Bank, and the European Community Grant HPRN-CT-2000–00082. We thank G. Pelster for excellent technical support.

Correspondence should be addressed to Jörg Striessnig, Institut für Pharmazie, Abteilung Pharmakologie und Toxikologie, Peter-Mayr-Strasse 1/I, A-6020 Innsbruck, Austria.

 0270-6474/03/236041-09$15.00/0

the synapses of the outer and inner plexiform layer as well as on photoreceptor cell bodies (Firth et al., 2001; Morgans, 2001; Morgans et al., 2001; Ball et al., 2002; Berntson et al., 2003). Its physiological relevance for normal retinal function is evident from $Ca_v1.4$ $\alpha1$ mutations causing incomplete X-linked congenital stationary night blindness (iCSNB2) in humans (Bech-Hansen et al., 1998; Strom et al., 1998). $Ca_v1.4\alpha1$ could therefore also represent a synaptically localized Ca^{2+} channel in the retina. However, this interpretation is complicated by the fact that $Ca_v1.4\alpha1$ is the only cloned mammalian Ca^{2+} channel $\alpha1$ subunit that has not yet been functionally characterized. Its characterization in isolated neurons is hampered by the lack of $Ca_v1.4\alpha1$-deficient mouse models. These would allow the identification of neurons, such as photoreceptors, with predominantly $Ca_v1.4\alpha1$-mediated currents and isolate them from the residual Ca^{2+} current components. In the absence of such models, the biophysical and pharmacological characterization of recombinant $Ca_v1.4\alpha1$ channels would allow us to address many open questions: can $Ca_v1.4\alpha1$ form DHP-sensitive LTCCs and $I_{Ca,L}$ as described in retinal neurons? Do its biophysical properties resemble $Ca_v1.2\alpha1$ or rather the lower voltage-activated $Ca_v1.3\alpha1$? Do $Ca_v1.4\alpha1$ currents exhibit Ca^{2+}-dependent inactivation? $Ca_v1.4\alpha1$ subunits lack a tyrosine in transmembrane segment IVS6, which was found previously to be part of the DHP-binding pocket of other LTCCs (Peterson et al., 1996; Striessnig et al., 1998). This raises the question of whether $Ca_v1.4\alpha1$ exhibits the typical DHP sensitivity by which retinal $I_{Ca,L}$ has been defined.

Here we describe for the first time the successful functional expression of a human retinal $Ca_v1.4\alpha1$ in mammalian cells. We show that $Ca_v1.4\alpha1$ channels share many of the properties of $Ca_v1.3\alpha1$, including intermediate DHP sensitivity, but lack Ca^{2+}-dependent inactivation under identical experimental conditions.

Materials and Methods

Cloning of human $Ca_V1.4\alpha1$ subunits. The $Ca_v1.4\alpha1$ cDNA (Strom et al., 1998) (GenBank AJ224874; open reading frame length, 5898 bp) was cloned from five subfragments (F1–F5) using different native or artificial restriction enzyme (RE) sites [nucleotide numbers (nt) are given in parentheses; asterisks indicate artificial RE sites introduced by PCR]: F1, *Sal*I*-*Bam*HI (nt, −5–812), F2, *Bam*HI-*Sph*I (nt, 812–1993), F3 *Sph*I-*Cla*I (nt, 1993–3255), F4, *Cla*I-*Eco*RI (nt, 3255–4349), F5, *Eco*RI-*Xba*I* (nt, 4349–5907). Fragments were generated by reverse transcriptase (RT)-PCR using proofreading *pfu* DNA polymerase (Stratagene, La Jolla, CA). First strand cDNA as a PCR template was synthesized from 1–1.5 μg of human retinal poly A^+ RNA (Clontech, Cambridge, UK) with the Ready-To-Go T-primed first-strand reaction kit (Amersham Biosciences, Arlington Heights, IL). PCR fragments were subcloned into vectors pBluescript SK+ (Stratagene) or pSport-1 (Invitrogen, San Diego, CA). Sequence integrity of the subclones was determined by DNA sequencing (MWG Biotech, Ebersberg, Germany). The construction of the complete $Ca_v1.4\alpha1$ was performed as follows: fragment F1 + 2 was generated by ligating the *Bam*HI-*Sph*I fragment (F2) into the corresponding RE sites of pSport-1-containing fragment F1. Fragment F4 + 5 was generated by ligating the *Cla*I-*Eco*RI fragment (F4) into the corresponding RE sites of pBluescript SK+-containing fragment F5. These steps were followed by a three fragment ligation of the *Sal*I*–*Sph*I fragment (F1 + 2) and the *Sph*I-*Cla*I fragment (F3) into the *Sal*I and *Cla*I sites of the F4 + 5-containing pBluescript SK+. For subsequent expression studies, the $Ca_v1.4\alpha1$ construct was either inserted into plasmid $pGFP^+$ (Grabner et al., 1998; Koschak et al., 2001) (yielding $Ca_v1.4\alpha1$ with GFP fused to its N terminus GFP-$Ca_v1.4\alpha1$) or into the corresponding vector $pGFP^-$, which lacks the GFP sequence.

Transient expression of LTCCs in tsA-201 cells. tsA-201 cells were maintained at 37°C and 5% CO_2 in DMEM–Coon's F12 medium (Invitrogen) supplemented with 10% (v/v) FCS (Sebak, Aidenbach, Germany), 2 mM L-glutamine, and 100 U/ml of penicillin streptomycin. For transient Ca^{2+} channel expression, cells were plated onto 10 cm tissue culture dishes 12 hr before transfection with Ca^{2+} phosphate precipitation using standard protocols. Human $Ca_v1.4\alpha1$, human $Ca_v1.3\alpha1$ (Koschak et al., 2001), human $Ca_v2.1\alpha1$ (Wappl et al., 2002), or rabbit $Ca_v1.2\alpha1$-a (Mikami et al., 1989) subunits were expressed together with $\alpha2\delta1$ (Ellis et al., 1988), rat $\beta3$ subunits (Castellano et al., 1993), or rat $\beta2a$ (Perez-Reyes et al., 1992). Transfection protocols for $Ca_v2.1\alpha1$, $Ca_v1.2\alpha1$, and $Ca_v1.3\alpha1$ subunits were as described previously (Koschak et al., 2001). $Ca_v1.4\alpha1$-transfected cells were incubated at 30°C and 5% CO_2 6–8 hr after transfection for 2–3 d before recording. One day before recording, cells were transferred to 3 cm culture dishes containing glass coverslips for drug application experiments. Transfected cells were visualized as GFP-$Ca_v1.4\alpha1$ or by cotransfected GFP fluorescence.

Membrane preparation and immunoblotting with affinity-purified sequence-directed antibodies. Immunoblotting was performed as described previously (Safayhi et al., 1997; Platzer et al., 2000) using a generic anti-$\alpha1$ sequence-directed antibody (anti-$\alpha1_{1382–1400}$; raised against residues 1382–1400 of $Ca_v1.1\alpha1$) (Safayhi et al., 1997). Membranes from tsA-201 cells transfected with 3 μg of $\alpha1$, 2 μg of β, 2.5 μg of $\alpha2\delta1$ subunit cDNA, and 2.5 μg of pUC18 carrier DNA in a 10 cm culture dish were prepared as described previously (Huber et al., 2000).

Electrophysiological recordings. Whole-cell patch-clamp experiments were performed at room temperature (Axopatch 200B amplifier; Axon Instruments, Foster City, CA) and linked to a personal computer equipped with pClamp version 7.0. Currents were recorded at sampling rates of 5 or 25 kHz and low-pass filtered at 2 or 5 kHz with a Digidata 1322A analog-to-digital board (Axon Instruments). Borosilicate glass pipettes were pulled using a Sutter P-97 (Linton Instruments, Palgrave, UK), microelectrode puller and fire polished, showing typical resistances of 2–3 MΩ when filled with internal solution. Capacitance compensation and series resistance compensations of 60% were used. The solutions for whole-cell measurements were as follows (in mM): (internal solution) 135 CsCl, 10 Cs-EGTA, and 1 $MgCl_2$, adjusted to pH 7.4, with CsOH; (recording solution) 15 $BaCl_2$ or 15 $CaCl_2$, 10 HEPES, 150 Choline-Cl, and 1 $MgCl_2$, adjusted to pH 7.4, with CsOH. The holding potential (HP) was −80 mV, unless stated otherwise. The presence of ATP in the pipette solutions did not affect run down of heterologously expressed L-type channels (see below) and was therefore omitted. All voltages were corrected for a liquid junction potential of −9 mV for Ba^{2+} and −8 mV for Ca^{2+}-containing solutions. Leak and capacitative currents were measured using hyperpolarizing pulses. Raw currents were corrected for linear leak currents. The voltage dependence of activation was determined from current–voltage (*I–V*) curves obtained by step depolarizations from the holding potential to various test potentials. *I–V* curves were fitted according to the following:

$$I = G_{max}(V - V_{rev})/(1 + \exp[(V_{0.5,act} - V)/k_{act}]), \quad (1)$$

where V_{rev} is the extrapolated reversal potential of I_{Ba}, V is the membrane potential, I is the peak current, G_{max} is the maximum conductance of the cell, $V_{0.5,act}$ is the voltage for half-maximal activation, and k_{act} is the slope factor of the Boltzmann term. The time course of current activation was fitted to the following exponential functions:

$$I(t) = A_0 \times \exp(-t/\tau_0) + C, \quad (2)$$

where $I(t)$ is the current at time t after the depolarization, A_0 the steady state current amplitude with the respective time constant of activation, τ_0, and C the remaining steady state current or to the following:

$$I(t) = A_{fast}[\exp(-t/\tau_{fast})] + A_{slow}[\exp(-t/\tau_{slow})] + C, \quad (3)$$

yielding time constants for a fast (τ_{fast}) and a slow (τ_{slow}) component.

Effects of DHPs were monitored continuously using 0.1 Hz depolarizing pulses (40 msec) to V_{max}. DHPs were dissolved in the recording solution from a 10 mM stock solution in dimethyl sulfoxide and perfused through a microcapillary onto cells using a gravity driven perfusion system. Only cells exhibiting stable currents (run down <5% during the first 60 sec) were used for analysis of DHP effects. The DHPs isradipine

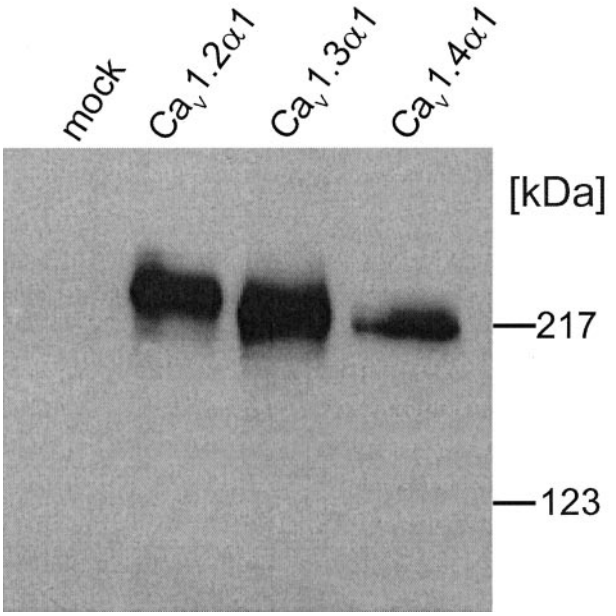

Figure 1. Heterologous expression of different LTCC subunits in tsA-201 cells. Cells were transfected with $Ca_v1.2\alpha1$, $Ca_v1.3\alpha1$, or $Ca_v1.4\alpha1$ together with $\beta3$ and $\alpha2\delta1$ subunit cDNA as described in Materials and Methods. Expression of $\alpha1$ subunit proteins was analyzed in immunoblots of membranes prepared from lyzed cells after separation on 8% SDS-PAGE gels (10 μg of membrane protein per lane) using a generic anti-$\alpha1$ sequence directed antibody (anti-$CP_{1382-1400}$). No $\alpha1$ immunoreactivity was present in mock-transfected cells used as a control. One of four experiments yielding similar results is shown.

and BayK 8644 (kindly provided by Novartis, Basel, Switzerland, and Bayer, Wuppertal, Germany) were used as their racemic mixtures.

Activation of G-proteins was achieved by intracellular perfusion with guanosine 5′-[γ-thio]triphoshate (GTPγS; Sigma, St. Louis, MO) for >3 min under whole-cell conditions. The degree of voltage-dependent current facilitation was determined as the ratio (facilitation ratio) of absolute peak current amplitudes before [−PP (prepulse)] and after (+PP) a conditioning prepulse (5–200 msec to voltages between 80 and 140 mV).

Statistics. Data were analyzed using Clampfit 8.0 (Axon Instruments) and Origin 5.0 (Microcal Software, Northampton, MA). All data are presented as mean ± SE for the indicated number of experiments. Statistical significance was determined by unpaired student's *t* test except when stated otherwise (Kruskal–Wallis test followed by Dunn's multiple comparison procedure, or one-way ANOVA followed by Bonferroni test as indicated).

Results

Although the DNA sequences of the human and mouse $Ca_v1.4\alpha1$ subunits are known (Bech-Hansen et al., 1998; Strom et al., 1998; Naylor et al., 2000), their successful functional expression has not been reported so far. We therefore constructed a full-length $Ca_v1.4\alpha1$ cDNA derived from human retina for functional expression in tsA-201 cells. The $Ca_v1.4\alpha1$ cDNA contains exons 1, 2, and 9a (Strom et al., 1998; Boycott et al., 2001).

We first confirmed the efficient expression of full-length $Ca_v1.4\alpha1$ subunits (calculated molecular mass, 220 kDa) on the protein level by immunoblot analysis of transfected tsA-201 cell membranes (Fig. 1). As expected for the full-length form of $Ca_v1.4\alpha1$, the immunostained band comigrated with the prestained myosin molecular mass standard (217 kDa), slightly faster than $Ca_v1.3\alpha1$ (calculated molecular mass, 242.5 kDa) and $Ca_v1.2\alpha1$ (Fig. 1). Its expression density was slightly lower than that of $Ca_v1.2\alpha1$ and $Ca_v1.3\alpha1$ (Fig. 1) ($n = 4$).

Next, we investigated whether the heterologously expressed $Ca_v1.4\alpha1$ subunits can also form functional channels after expression in tsA-201 cells using the whole-cell patch-clamp technique. Using a standard transfection protocol and cotransfection with $\alpha2\delta1$ and $\beta3$ subunits, significant I_{Ba} was measurable during depolarization from an HP of −90 mV for both $Ca_v1.4\alpha1$ and the GFP-$Ca_v1.4\alpha1$ fusion protein (Fig. 2). Compared with $Ca_v1.3\alpha1$, the expression efficiency was lower. Only 50 of 227 (22%) $Ca_v1.4\alpha1 + \beta3 + \alpha2\delta1$ and 19 of 71 (28%) GFP-$Ca_v1.4\alpha1 + \beta3 + \alpha2\delta1$ transfected (i.e., GFP-positive) cells yielded I_{Ba} (15 mM Ba^{2+} as charge carrier), exceeding endogenous currents (Fig. 2, legend). In contrast, 66% of GFP-positive cells transfected with $Ca_v1.3\alpha1 + \beta3 + \alpha2\delta1$ (and >90% with $Ca_v1.2\alpha1 + \beta3 + \alpha2\delta1$; data not shown) expressed L-type currents. When $Ca_v1.4\alpha1$ was coexpressed with $\beta3$ subunits in the absence of $\alpha2\delta1$, current densities did not exceed those of endogenous currents measured in untransfected tsA-201 cells (Fig. 2*A*) ($p > 0.05$). This shows that $Ca_v1.4\alpha1$ can associate with $\alpha2\delta$ subunits. Because β subunits exert modulatory effects on $Ca_v1.4\alpha1$-meditated currents (see below), the smallest functional complex is $Ca_v1.4\alpha1 + \beta + \alpha_2\delta$. Coexpression of $Ca_v1.4\alpha1 + \alpha2\delta1$ with $\beta2a$ subunits, which are important for normal retinal function (Ball et al., 2002), also yielded significant I_{Ba} above endogenous currents ($p < 0.01$) (Fig. 2*A*).

We analyzed the biophysical properties of $Ca_v1.4\alpha1$-mediated currents in comparison with $Ca_v1.2\alpha1$ and $Ca_v1.3\alpha1$, which, like $Ca_v1.4\alpha1$, are also expressed in sensory cells including the retina

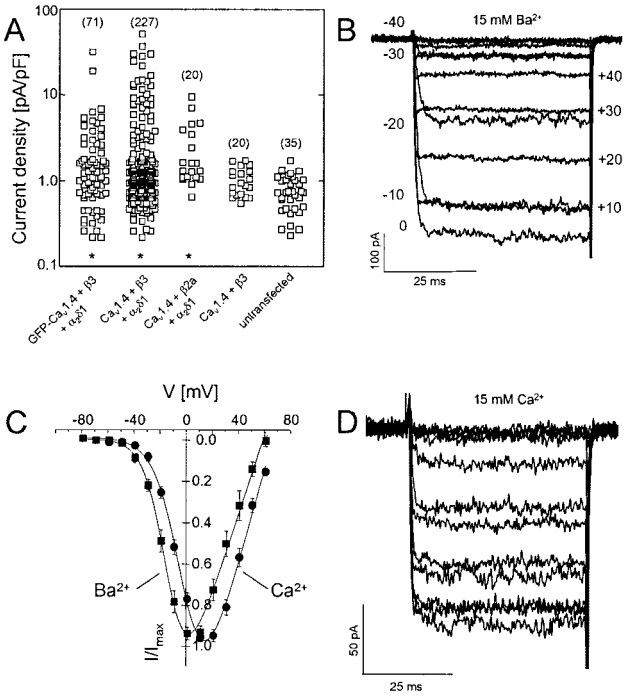

Figure 2. Biophysical properties of I_{Ba} and I_{Ca} through $Ca_v1.4\alpha1$ subunits. $Ca_v1.4\alpha1$ subunits were expressed together with $\beta3 + \alpha2\delta1$ (*A–C*) or $\beta2a + \alpha2\delta1$ (*A*), as described in Materials and Methods, using 15 mM Ba^{2+} (*A–C*) or 15 mM Ca^{2+} (*D*) as charge carrier. *A*, Expression density was determined by depolarizing pulses to V_{max}. I_{Ba} was measured 48 – 82 hr after transfection for the indicated number of cells. Small currents measured in untransfected cells were attributable to endogenous non-L-type currents that were <1.72 pA/pF. Asterisks indicate statistically significant difference to untransfected cells ($p < 0.01$; Kruskal–Wallis test, followed by Dunn's multiple comparison test). *B*, Superimposed currents were activated by depolarizing $Ca_v1.4\alpha1$-transfected cells during 50 msec pulses from an HP of −90 mV to between −60 and 40 mV in 10 mV steps. *C*, Normalized *I–V* curves for $Ca_v1.4\alpha1$ coexpressed with $\beta3$ and $\alpha2\delta1$ subunits using 15 mM Ba^{2+} (black squares) or Ca^{2+} (black circles) as charge carriers. Biophysical parameters are given in Table 1. *D*, Protocol as in *B* but with 15 mM Ca^{2+} in the bath solution.

Table 1. Biophysical properties of Ba^{2+} and Ca^{2+} currents through heterologously expressed $Ca_v1.4\alpha1$ subunits

Subunits coexpressed with $\alpha2\delta1$	Charge carrier (mM)	$V_{0.5,act}$ (mV)	k_{act} (mV)	V_{max} (mV)	Activation threshold (mV)	Current density (pA/pF)	+ BayK 8644 $V_{0.5,act}$ (mV)	+ BayK 8644 k_{act} (mV)
$Ca_v1.4\alpha1 + \beta3$	$15Ba^{2+}$	-8.9 ± 0.8	-8.0 ± 0.4	4.2 ± 0.7	-38.8 ± 0.7	15.5 ± 2.0	-21.5 ± 1.3^{xxx}	-5.7 ± 0.3^{xx}
		$n = 36$	$n = 36$	$n = 36$	$n = 36$	$n = 36$	$n = 9$	$n = 9$
GFP-$Ca_v1.4\alpha1 + \beta3$	$15Ba^{2+}$	-11.0 ± 1.4	-9.1 ± 0.4	2.7 ± 1.1	-42.0 ± 1.1	6.0 ± 1.8	-24.9 ± 1.5^{xxx}	-4.7 ± 0.5^{xxx}
		$n = 18$	$n = 18$	$n = 18$	$n = 18$	$n = 18$	$n = 8$	$n = 8$
$Ca_v1.4\alpha1 + \beta2a$	$15Ba^{2+}$	-10.7 ± 1.4	-9.5 ± 0.3	2.6 ± 1.3	$-45.6 \pm 1.2^{**}$	4.6 ± 1.3		
		$n = 6$	$n = 6$	$n = 6$	$n = 6$	$n = 6$	ND	ND
$Ca_v1.3\alpha1 + \beta3$	$15Ba^{2}$	$-16.8 \pm 0.7^{***}$	-9.2 ± 0.2	$-1.7 \pm 0.7^{***}$	$-44.5 \pm 0.5^{***}$	22.4 ± 4.2		
		$n = 52$	$n = 52$	$n = 52$	$n = 52$	$n = 52$	ND	ND
$Ca_v1.2\alpha1 + \beta3$	$15Ba^{2}$	$-3.0 \pm 1.1^{**}$	-8.0 ± 0.2	$13.4 \pm 1.9^{***}$	$-31.5 \pm 0.5^{***}$	20.4 ± 5.6		
		$n = 20$	$n = 20$	$n = 20$	$n = 20$	$n = 20$	ND	ND
$Ca_v1.4\alpha1 + \beta3$	$15Ca^{2+}$	$0.6 \pm 2.2^{**}$	-9.4 ± 0.5	$15.1 \pm 2.2^{***}$	-33.6 ± 1.8	12.7 ± 3.7		
		$n = 6$	$n = 6$	$n = 6$	$n = 6$	$n = 6$	ND	ND
$Ca_v1.3\alpha1 + \beta3$	$15Ca^{2}$	-7.8 ± 1.1	-9.4 ± 0.4	$7.1 \pm 1.6^{*}$	-37.3 ± 0.9	13.5 ± 2.2		
		$n = 13$	$n = 13$	$n = 13$	$n = 13$	$n = 13$	ND	ND
$Ca_v1.2\alpha1 + \beta3$	$15Ca^{2}$	$9.2 \pm 1.5^{+}$	$-10.5 \pm 0.3^{***}$	21.4 ± 1.2	$-27.6 \pm 1.3^{+}$	10.4 ± 2.1		
		$n = 22$	$n = 22$	$n = 22$	$n = 22$	$n = 22$	ND	ND

GFP-$Ca_v1.4\alpha1$ and $Ca_v1.4\alpha1$ Ca^{2+} channels were coexpressed with rat $\beta3$ or rat $\beta2a$ and rabbit $\alpha2\delta1$ subunits in tsA-201 cells, and the biophysical properties were determined using 15 mM Ba^{2+} or Ca^{2+} as a charge carrier. $V_{0.5,act}$, k_{act}, and V_{max} were obtained by fitting the data as described in Materials and Methods. The activation threshold was determined as the test potential at which 5% of the maximal current was activated. Data are given as means ± SE; ND, not determined. Statistical differences for $V_{0.5,act}$, k_{act}, V_{max}, and activation thresholds (calculated by one-way ANOVA, followed by Bonferroni test) are given in comparison with $Ca_v1.4\alpha1 + \beta3 + \alpha2\delta1$ with Ba^{2+} (*$p<0.05$; **$p<0.01$; ***$p<0.001$) or Ca^{2+} ($^{+}p<0.05$; $^{++}p<0.01$; $^{+++}p<0.001$) as charge carrier. For cells used for the calculation of biophysical parameters, current densities (no BayK 8644 present) are also given. For statistical comparisons of current densities, see Figure 2*A*. Statistically significant differences for BayK 8644 effects ($^{xx}p<0.01$; $^{xxx}p<0.001$; Student's *t* tests) are also indicated.

(Morgans et al., 1998; Taylor and Morgans, 1998; Morgans, 1999; Berntson et al., 2003). $Ca_v1.4\alpha1$ I_{Ba} typically activated at more negative voltages (-38.8 ± 0.7 mV; $n = 36$; $\beta3 + \alpha2\delta1$ coexpression) than $Ca_v1.2\alpha1$ but slightly more positive than $Ca_v1.3\alpha1$ ($p < 0.001$) (Table 1) (Koschak et al., 2001). Representative currents activated by 50 msec step depolarizations to different test potentials (HP, −90 mV) are illustrated in Figure 2*B*. The *I–V* relationship ($V_{0.5,act}$, V_{max}) was shifted to more positive potentials with 15 mM Ca^{2+} as the charge carrier ($p < 0.01$) (Table 1, Fig. 2*C*).

The time course of activation determined during 50 msec depolarizations to V_{max} revealed similar activation time constants for I_{Ba} through GFP-tagged or non-GFP-tagged $Ca_v1.4\alpha1$ subunits. When coexpressed with $\beta3 + \alpha2\delta1$, activation could be described by a monoexponential time course in the majority of cells ($Ca_v1.4\alpha1$; 0.43 ± 0.08 msec; 9 of 14 cells). In the remaining cells, a biexponential onset of activation was measured ($\tau_{fast} = 0.46 \pm 0.08$ msec; $\tau_{slow} = 16.4 \pm 3.9$ msec; relative contribution of slow component, $6.03 \pm 1.93\%$). Coexpression of $\beta2a$ subunits primarily resulted in activation by a biexponential time course (three of four cells; $\tau_{fast} = 0.70 \pm 0.13$ msec; $\tau_{slow} = 6.6 \pm 0.1$ msec; relative contribution of slow component, $3.9 \pm 1.1\%$). Therefore, with respect to the activation properties, I_{Ba} through $Ca_v1.4\alpha1$ Ca^{2+} channels closely resembled $Ca_v1.3\alpha1$ currents, which also activate with faster time courses and at lower voltages than $Ca_v1.2$ (Koschak et al., 2001; Scholze et al., 2001; Xu and Lipscombe, 2001). No changes in the (monoexponential) activation time course were detected for $Ca_v1.3\alpha1$ currents in the presence of $\beta2a$ subunits (monophasic activation; $\alpha2\delta1 + \beta3$, $\tau_{act} = 0.77 \pm 0.06$; $n = 24$; $\alpha2\delta1 + \beta2a$, $\tau_{act} = 0.73 \pm 0.1$; $n = 4$; $p > 0.05$).

One property that distinguishes $Ca_v1.3\alpha1$ from $Ca_v1.2\alpha1$ currents is its slower inactivation during prolonged depolarizations (Koschak et al., 2001). The experiments in Figure 3 illustrate that inactivation of $Ca_v1.4\alpha1$ was even slower than for $Ca_v1.3\alpha1$ (Fig. 3). Only $50.2 \pm 2.9\%$ ($n = 17$) of I_{Ba} inactivated after 5 sec of depolarization to V_{max} (Fig. 3*A*,*B*). After 10 sec, $84.2 \pm 6.4\%$ ($n = 4$) of $Ca_v1.3\alpha1$ but only $68.1 \pm 2.7\%$ ($n = 17$) of $Ca_v1.4\alpha1$ I_{Ba} inactivated ($p < 0.05$) (Fig. 3*A*,*B*). Substitution of $\beta2a$ for $\beta3$ subunits also significantly slowed inactivation (Fig. 3*E*,*F*). This also demonstrates that β subunits participate in fine tuning the $Ca_v1.4\alpha1$ channel complex.

In addition to voltage, Ca^{2+} is also an important determinant of LTCC inactivation. Figure 3, *C* and *D*, illustrates that not only inactivation of $Ca_v1.2\alpha1$ (for review, see Budde et al., 2002) but also of heterologously expressed $Ca_v1.3\alpha1$ occurred in a Ca^{2+}-dependent manner (percentage of current inactivation after 250 msec; $Ca_v1.2\alpha1$, I_{Ba}, $60.7 \pm 8\%$; $n = 4$; I_{Ca}, $84.5 \pm 3.1\%$; $n = 6$; $p < 0.05$; $Ca_v1.3\alpha1$, I_{Ba}, $37.5 \pm 2.9\%$; $n = 13$; I_{Ca}, $68.8 \pm 4.7\%$; $n = 12$; $p < 0.001$). In contrast, under the same experimental conditions (10 mM EGTA in the pipette solution), $Ca_v1.4\alpha1$ did not exhibit accelerated inactivation with Ca^{2+} as charge carrier throughout its slow inactivation time course (Fig. 3*A*,*B*). As a consequence, the majority of I_{Ca} through $Ca_v1.2\alpha1$ and $Ca_v1.3\alpha1$, but hardly any $Ca_v1.4\alpha1$ current, inactivated during 200–400 msec.

LTCCs are defined by their high sensitivity to DHP antagonists and their activation by DHP Ca^{2+} channel activators (Peterson et al., 1996), such as BayK 8644. In $Ca_v1.4\alpha1$ subunits, a IVS6 tyrosine (position 1414 in the human $Ca_v1.4\alpha1$ sequence) (Fig. 8), previously shown to contribute to the formation of the binding pocket (Peterson et al., 1996), is replaced by a phenylalanine. The corresponding mutation in $Ca_v1.1\alpha1$ subunits reduces DHP antagonist sensitivity ~3- to 5-fold (Peterson et al., 1996). Its role for agonist action has not yet been studied. Therefore, we tested the DHP sensitivity of heterologously expressed $Ca_v1.4\alpha1$ channels ($+ \beta3 + \alpha2\delta1$). At −90 mV HP, the DHP antagonist isradipine (1 μM) blocked $82.7 \pm 2.9\%$ ($n = 7$) of I_{Ba} elicited by 0.1 Hz depolarizing pulses to V_{max} (Fig. 4*A*). The same concentration completely inhibited $Ca_v1.3\alpha1$ currents under identical experimental conditions, as reported previously (Koschak et al., 2001) (Fig. 4*B*). Current inhibition by 300 nM concentrations was also slightly less pronounced for $Ca_v1.4\alpha1$, compared with $Ca_v1.3\alpha1$ (Koschak et al., 2001) (Fig. 4*B*). Changing the HP from −90 to −50 mV dramatically increased isradipine sensitivity of $Ca_v1.4\alpha1$ (Fig. 4*B*, open triangle), indicating a voltage-dependent mechanism of DHP block, which is also typical for both $Ca_v1.2\alpha1$ and $Ca_v1.3\alpha1$ (Welling et al., 1997; Koschak et al., 2001). Activation of I_{Ba} through $Ca_v1.4\alpha1$ by the Ca^{2+} channel activator BayK 8644 occurred in an LTCC-typical manner (Fig. 5). Perfusion of

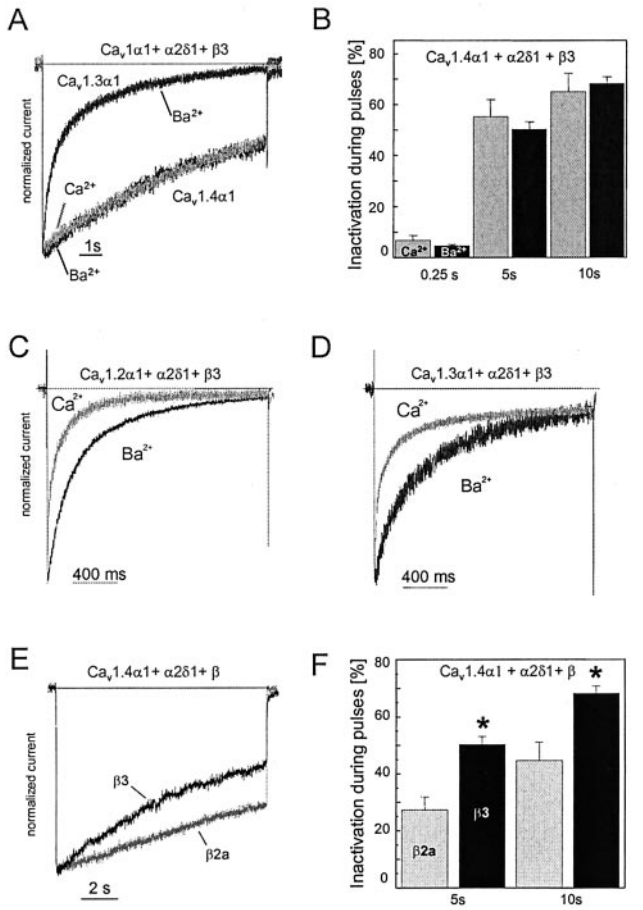

Figure 3. Inactivation properties of $Ca_v1.4\alpha1$ Ca^{2+} channels. *A*, I_{Ba} (black traces) through $Ca_v1.3\alpha1$ and $Ca_v1.4\alpha1$ subunits coexpressed with $\beta3$ and $\alpha2\delta1$ subunits were elicited by 10 sec depolarizing pulses from an HP of −90 mV to V_{max}. Representative current traces for $Ca_v1.3\alpha1$ ($n = 4$) and $Ca_v1.4\alpha1$ ($n = 17$) channels are shown. Traces were normalized to the peak current amplitudes. For the experiments shown, inactivation measured during 5 and 10 sec depolarizing pulses was as follows: $Ca_v1.4\alpha1$, 41 and 56%; $Ca_v1.3\alpha1$, 89 and 97%. A representative trace for current through $Ca_v1.4\alpha1$ recorded with 15 mM Ca^{2+} as charge carrier is illustrated in gray superimposed on the I_{Ba} trace indicated in black. *B*, Percent current inactivation measured after 0.25, 5, and 10 sec depolarizations to V_{max} in $Ca_v1.4\alpha1$-transfected cells using either 15 mM Ba^{2+} or 15 mM Ca^{2+} as the charge carrier. Inactivation of currents during pulses was not significantly different for Ba^{2+} (black bars) and Ca^{2+} (gray bars) ($n = 7$; $p > 0.05$). *C*, *D*, Inactivation for $Ca_v1.2\alpha1$ (*C*) and $Ca_v1.3\alpha1$ (*D*) during 2 sec depolarizing pulses to V_{max} with 15 mM Ba^{2+} (black trace) or 15 mM Ca^{2+} (gray trace) as charge carriers. For $Ca_v1.3\alpha1$, a variable noninactivating I_{Ca} component was found (9–40%; $n = 4$), whereas remaining $Ca_v1.2\alpha1$ currents were always <3.5% ($n = 7$). *E*, Inactivation of I_{Ba} through $Ca_v1.4\alpha1$ cotransfected with $\beta3$ (black) or $\beta2a$ (gray) and $\alpha2\delta1$. Currents were normalized to peak I_{Ba}. Currents were elicited by depolarization from an HP of −90 mV to V_{max}. *F*, Percentage of inactivation of I_{Ba} through $Ca_v1.4\alpha1$ cotransfected with $\beta3$ (black; $n = 17$) or $\beta2a$ (gray; $n = 7$), and $\alpha2\delta1$ was determined after 5 and 10 sec during a depolarization from an HP of −90 mV to V_{max}. Currents were normalized to peak I_{Ba}. Inactivation with $\beta2a$ coexpression was 27.2 ± 4.6% (after 5 sec) and 44.6 ± 6.4% (after 10 sec; $n = 7$), respectively. Asterisks indicate a statistically significant difference to $\beta2a$ coexpression ($p < 0.01$).

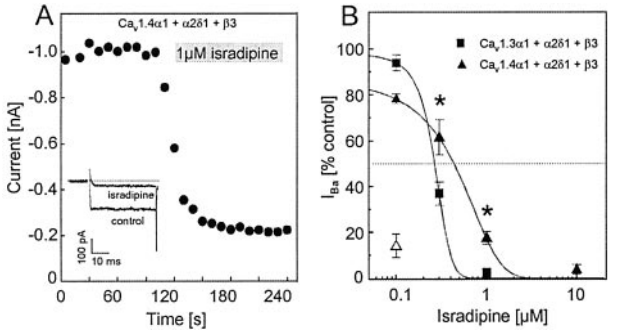

Figure 4. DHP antagonist sensitivity of $Ca_v1.4\alpha1$ Ca^{2+} channels. $Ca_v1.4\alpha1$ was coexpressed with $\beta3$ and $\alpha2\delta1$ subunits in tsA-201 cells and recorded in bath solution containing 15 mM Ba^{2+} as charge carrier. *A*, I_{Ba} was elicited from depolarizations to V_{max} (filled circles) in the absence or presence (gray bar) of the DHP antagonist isradipine. For the experiment shown, I_{Ba} block by 1 μM isradipine was 80%. Corresponding peak current traces elicited by 40 msec depolarizations in the absence (control) and presence of isradipine are shown in the inset. *B*, Concentration-dependent inhibition was measured from a holding potential of −90 mV for $Ca_v1.4\alpha1$ (black triangles) during superfusion of the cell with bath solution containing the indicated concentrations of isradipine. The dose–response relationship was compared with $Ca_v1.3\alpha1$ (squares) (Koschak et al., 2001). Pronounced voltage dependence of isradipine block of I_{Ba} through $Ca_v1.4\alpha1$ subunits was observed by changing the HP from −90 to −50 mV (open triangle). Asterisks indicate statistically significant difference ($p < 0.05$; data are means ± SE).

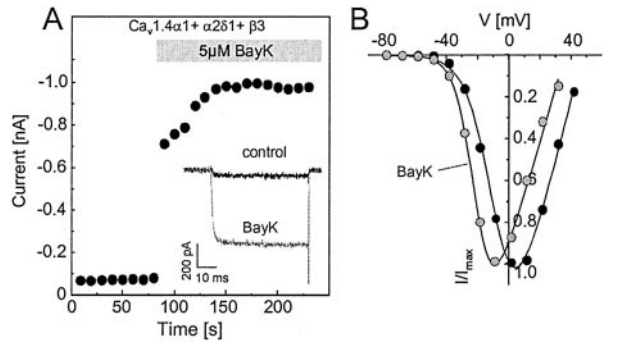

Figure 5. DHP agonist sensitivity of $Ca_v1.4\alpha1$ Ca^{2+} channels. For all experiments, $Ca_v1.4\alpha1$ subunits were coexpressed with $\beta3$ and $\alpha2\delta1$ subunits in tsA-201 cells. Charge carrier was 15 mM Ba^{2+}. One representative experiment (of 9) is shown. *A*, Stimulation of I_{Ba} through $Ca_v1.4\alpha1$ Ca^{2+} channels by the Ca^{2+} channel activator BayK 8644 (BayK). I_{Ba} was elicited by depolarizations to V_{max} before and after application of BayK 8644-containing solution (5 μM). Maximal I_{Ba} is plotted against time. The inset shows representative traces in the absence (control) and presence of BayK 8644. *B*, Current–voltage relationship for $Ca_v1.4\alpha1$ in the absence (black circles) and presence of 5 μM BayK 8644 (BayK; gray circles). $V_{0.5,act}$ was −8 and −21.1 mV for the control and BayK 8644-modulated current, respectively. One representative experiment (of 7) is shown.

$Ca_v1.4\alpha1$-transfected cells (yielding significant I_{Ba} already in the absence of drug) with 5 μM BayK 8644 resulted in a robust (9.6 ± 1.9-fold; $n = 7$) increase of the maximal I_{Ba} (Fig. 5*A*), similar to $Ca_v1.3\alpha1$ stimulation (Koschak et al., 2001). Furthermore, BayK 8644 produced a typical ~10 mV hyperpolarizing shift of the *I–V* curve (Table 1, Fig. 5*B*). Interestingly, in some GFP-positive cells (four of four tested) with no significant current under basal conditions, the presence of $Ca_v1.4\alpha1$ currents was unmasked by application of the Ca^{2+} channel activator BayK 8644 (5 μM; 10.5 ± 1.3 pA/pF; $n = 4$). This suggested that an even >10-fold stimulation of $Ca_v1.4\alpha1$ currents occurred in some cells. Interestingly, a similarly strong BayK 8644 dependence of L-type current components has also been described in retinal cone bipolar cells (Pan, 2000). Our data demonstrate that phenylalanine in position 1414 of $Ca_v1.4\alpha1$ still supports full agonist sensitivity. Therefore, a tyrosine in this position is unlikely to be required for DHP agonist action in LTCCs.

We also tested the modulation of $Ca_v1.4\alpha1$ currents by G-protein activation and/or strong depolarizing pulses. Figure 6*A* shows the effect of 200 msec depolarizing prepulses to 80 mV on I_{Ba} through $Ca_v1.4\alpha1$, elicited by a subsequent test pulse to V_{max}. Prepulses facilitated I_{Ba} in 59% (10 of 17) of $Ca_v1.4\alpha1 + \beta3 + \alpha2\delta1$-transfected cells. The absence of facilitation in some cells has also been reported previously for $Ca_v1.2\alpha1$ after expression in

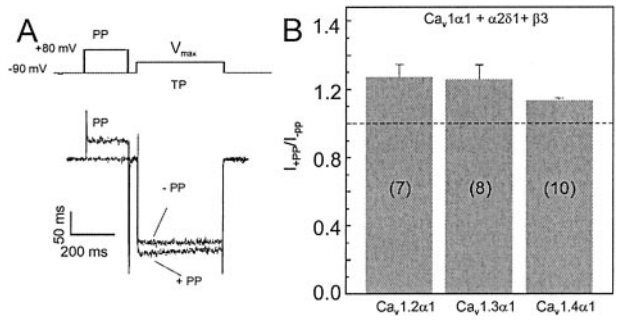

Figure 6. Voltage-dependent facilitation of $Ca_v1.4\alpha1$ subunits. *A*, Schematic representation of the voltage protocol used to elicit facilitation. Channel activity was recorded in tsA-201 cells transfected with $Ca_v1.4\alpha1$, $\beta3$, and $\alpha_2\delta1$ subunits in 15 mM Ba^{2+} solution. Test pulses (TPs) of 400 msec were applied with or without a 200 msec PP. A representative current trace (facilitation ratio, 1.11) is shown. Note the differences in activation and inactivation kinetics time courses. *B*, Comparison of voltage-dependent facilitation of different LTCCs. Facilitation of $Ca_v1.2\alpha1$, $Ca_v1.3\alpha1$, and $Ca_v1.4\alpha1$ I_{Ba} is expressed as the amplitude ratio of currents recorded with a prepulse (+PP) over the respective control currents without prepulse (−PP). A similar extent of facilitation was observed for all LTCC subtypes tested ($p > 0.05$). Facilitation was observed in seven of seven $Ca_v1.2\alpha1$-transfected cells, eight of 20 $Ca_v1.3\alpha1$-transfected cells, and 10 of 17 $Ca_v1.4\alpha1$ ($+ \beta3 + \alpha2\delta1$)-transfected cells.

mammalian cells (Kamp et al., 2000). In cells showing facilitation, the extent of facilitation was slightly (but not significantly) smaller for $Ca_v1.4\alpha1$ (facilitation ratio, 1.13 ± 0.02) than for $Ca_v1.2$ $\alpha1$ (1.27 ± 0.07) and $Ca_v1.3$ $\alpha1$ (1.26 ± 0.09) (Fig. 6*B*) when measured under identical experimental conditions. As expected (Bourinet et al., 1994), no facilitation was observed for the P/Q-type channel $Ca_v2.1\alpha1$ subunit (Fig. 7*B*,*C*, lower panel) ($n = 7$) under these experimental conditions. The application of 200 msec prepulses not only increased the peak current but also accelerated the activation and inactivation kinetics of the facilitated $Ca_v1.4\alpha1$ current (Fig. 6*A*). Whereas control I_{Ba} hardly inactivated (>97% of current remained at the end of the 400 msec test pulse) (Fig. 6*A*), slightly accelerated inactivation was detected for the facilitated current (92.8 ± 0.8% residual current; $p < 0.001$). Similar kinetic changes have also been observed for other facilitated L-type currents (Dai et al., 1999; Kamp et al., 2000). Coexpression with $\beta2a + \alpha2\delta1$ subunits also supported facilitation, which was observed in 85% of the experiments, and the average facilitation ratio was similar, as measured for $\beta3 + \alpha2\delta1$ (1.18 ± 0.03; $n = 6$). Similar facilitation was observed with Ca^{2+} as a charge carrier. Prepulses facilitated I_{Ca} in five of five $Ca_v1.4\alpha1 + \beta3 + \alpha2\delta1$-transfected cells (facilitation ratio, 1.16 ± 0.06).

We found no evidence for a G-protein dependence of this prepulse facilitation of $Ca_v1.4\alpha1$ currents. When the nonhydrolyzable GTP analog GTPγS was included in the pipette solution to activate expressed G-proteins in tsA-201 cells (Herlitze et al., 1997; Meza and Adams, 1998), facilitation induced by 5 msec depolarizing prepulses to 140 mV remained unaffected (Fig. 7). To prove that G-protein activation is feasible under our experimental conditions, the modulation of $Ca_v2.1\alpha1$ channels was determined using the same experimental protocol. At least 3 min after establishing the whole-cell configuration, prepulse application caused the typical relief of G-protein modulation of $Ca_v2.1\alpha1$ currents characterized by faster activation and the reduction of peak current amplitude (Fig. 7*B*,*C*). All $Ca_v2.1\alpha1 + \beta3 + \alpha2\delta1$-expressing cells (seven of seven) dialyzed with GTPγS exhibited this typical G-protein-mediated inhibition (Fig. 7*B*,*C*), consistent with previous studies (Bourinet et al., 1996; Zhang et al., 1996; Herlitze et al., 1997; Meza and Adams, 1998; Canti et al., 1999). These experiments clearly demonstrated that voltage-dependent G-protein modulation can be measured under our experimental conditions, but that facilitation of $Ca_v1.4\alpha1$ is unlikely to result from relief of G-protein-induced channel inhibition.

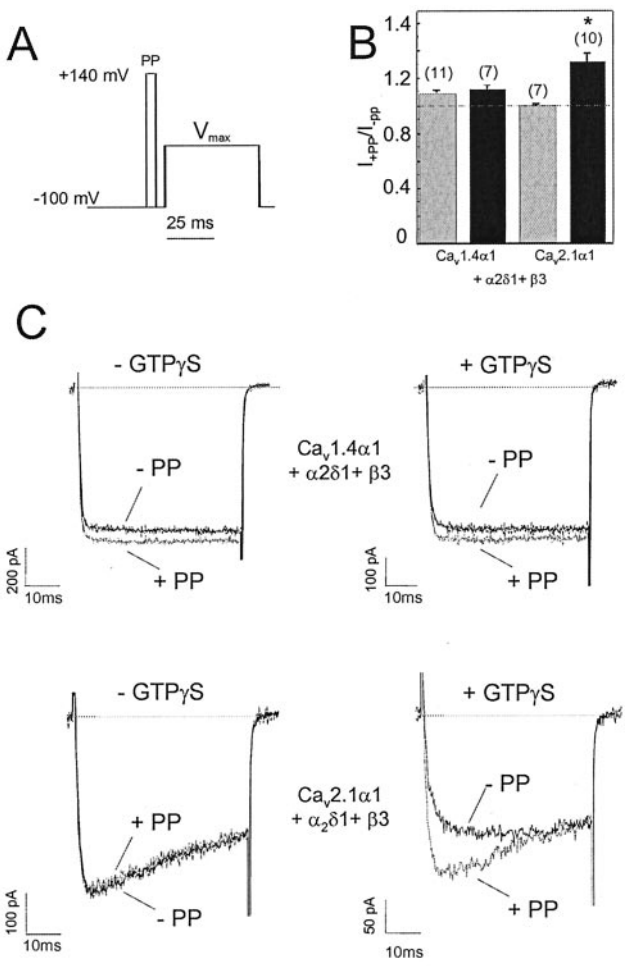

Figure 7. Depolarization-induced facilitation of $Ca_v1.4\alpha1$ subunits. *A*, Pulse protocol used to determine G-protein modulation of $Ca_v1.4\alpha1$- and $Ca_v2.1\alpha1$-mediated I_{Ba}. Facilitation was measured during 50 msec test pulses (TP) to V_{max} either with or without a 5 msec PP to 140 mV. *B*, Facilitation ratios for $Ca_v1.4\alpha1$ and $Ca_v2.1\alpha1$ Ca^{2+} channels (coexpressed with $\beta3$ and $\alpha2\delta1$) in the absence (control; gray bars) and presence of 300 μM intracellular GTPγS (black bars) using the pulse protocol described in *A*. Recordings were started after ≥3 min of dialysis with GTPγS. The following facilitation ratios were obtained in the absence and presence of GTPγS, respectively: $Ca_v1.4\alpha1$, 1.1 ± 0.02 ($n = 11$ of 17 cells), 1.12 ± 0.02 ($n = 7$ of 14 cells); $Ca_v2.1\alpha1$, 0.99 ± 0.01 ($n = 7$ of 7 cells), 1.3 ± 0.07 ($n = 10$ of 10 cells). Asterisk indicates statistically significant difference ($p < 0.01$). *C*, Representative current traces for the experiments described in *B*.

Discussion

Biophysical properties of $Ca_v1.4\alpha1$

Here we report the first successful functional characterization of Ca^{2+} currents through $Ca_v1.4\alpha1$ subunits. Experiments were performed under the same conditions previously used to compare the biophysical and pharmacological properties of $Ca_v1.3\alpha1$ and $Ca_v1.2\alpha1$ LTCCs using the whole-cell patch-clamp technique. $Ca_v1.4\alpha1$ currents resemble more closely $Ca_v1.3\alpha1$ than $Ca_v1.2\alpha1$. Like $Ca_v1.3\alpha1$, $Ca_v1.4\alpha1$ activated more rapidly and at more negative voltages than heterologously expressed $Ca_v1.2\alpha1$ and also inactivated more slowly. $Ca_v1.4\alpha1$ exhibited no Ca^{2+}-induced inactivation, which was found to exist in $Ca_v1.3\alpha1$ (Xu

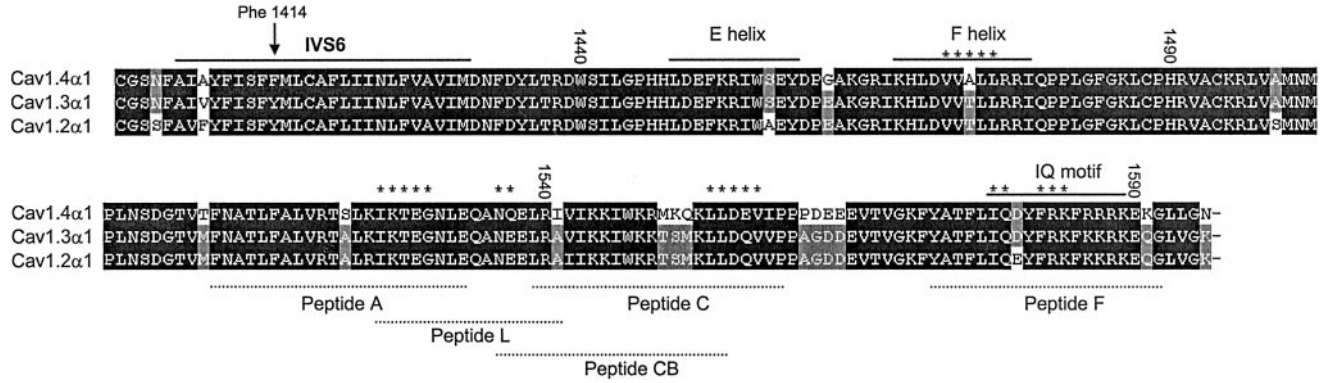

Figure 8. Sequence alignment of L-type $Ca_v1.4\alpha1$ with $Ca_v1.2\alpha1$ and $Ca_v1.3\alpha1$. An amino acid exchange within the proposed DHP-binding domain of LTCCs is indicated by an arrow. A tyrosine residue conserved in all L-type $\alpha1$ subunits is replaced by phenylalanine in position 1414 of $Ca_v1.4\alpha1$. The sequence alignment also illustrates amino acid differences between $Ca_v1.4\alpha1$ and $Ca_v1.2\alpha1$ or $Ca_v1.3\alpha1$, which might explain the differences in Ca^{2+}-dependent inactivation described under our experimental conditions. Sequence stretches previously identified as critical determinants for calmodulin-binding and Ca^{2+}-dependent inactivation (de Leon et al., 1995; Zuhlke et al., 1999; Mouton et al., 2001; Pitt et al., 2001) are indicated.

and Lipscombe, 2001; our observations) and is well studied for $Ca_v1.2\alpha1$ (for review, see Budde et al., 2002). Therefore, the slower inactivation of $Ca_v1.4\alpha1$ became especially prominent when Ca^{2+} was the permeating cation (Fig. 3).

Ca^{2+}-dependent inactivation is mediated through Ca^{2+} and calmodulin interaction with the C-terminal tail and is a typical property of LTCCs (for review, see Budde et al., 2002). However, the absence of Ca^{2+}-dependent inactivation is not a specific property of $Ca_v1.4\alpha1$. A putative neuronal $Ca_v1.2\alpha1$ C-terminal splice variant, $Ca_v1.2\alpha1_{86}$ ($\alpha1C_{,86}$), also lacks Ca^{2+}-induced inactivation (Soldatov et al., 1997). In this splice variant, 80 amino acid residues of the C-terminal tail are replaced by 81 essentially nonidentical amino acid residues. This eliminates important motifs essential for calmodulin-mediated Ca^{2+}-dependent inactivation and also causes a profound acceleration of voltage-dependent inactivation of I_{Ba}. In contrast, inspection of the $Ca_v1.4\alpha1$ sequence (Fig. 8) revealed that the regions recently identified as determinants for Ca^{2+}-dependent inactivation in $Ca_v1.2\alpha1$ (Qin et al., 1999; Zuhlke et al., 1999; Pate et al., 2000; Peterson et al., 2000; Romanin et al., 2000; Mouton et al., 2001; Pitt et al., 2001) are highly conserved in this subunit. Only a few amino acid differences, as compared with $Ca_v1.2\alpha1$ and $Ca_v1.3\alpha1$, exist in the F-helix of the EF hand (Peterson et al., 2000), peptide A (Pitt et al., 2001), the CB peptide (Pate et al., 2000), and peptide C (Pitt et al., 2001). Therefore, $Ca_v1.4\alpha1$ subunits represent an ideal model to further study the role of these amino acid changes for the molecular mechanisms of Ca^{2+}-dependent inactivation. Additional studies must also address the question whether $Ca_v1.4\alpha1$ undergoes N-lobe calmodulin-mediated calcium-dependent inactivation revealed at low intracellular Ca^{2+} buffering (Liang et al., 2003).

DHP-sensitivity of $Ca_v1.4\alpha1$

As for $Ca_v1.3\alpha1$, the apparent DHP antagonist sensitivity of $Ca_v1.4\alpha1$ was significantly lower (~15-fold) than for $Ca_v1.2\alpha1$ at negative holding potentials. This intermediate DHP antagonist sensitivity of $Ca_v1.4\alpha1$ and $Ca_v1.3\alpha1$ is in good accordance with data obtained on L-type currents in retinal cells, in which relatively high concentrations of DHPs are required to block $I_{Ca,L}$ (Wilkinson and Barnes, 1996; Protti and Llano, 1998; Taylor and Morgans, 1998). $Ca_v1.4\alpha1$ current inhibition by DHP antagonist was highly voltage dependent. At a more positive membrane potential, 100 nM isradipine inhibited >80% of I_{Ba} (Fig. 4*B*), indistinguishable from the block of $Ca_v1.3\alpha1$ under the same experimental conditions (Koschak et al., 2001). Therefore, the low apparent affinity of $Ca_v1.4\alpha1$ in comparison with $Ca_v1.2\alpha1$ is likely to be attributable to differences in the voltage-dependent interaction of the DHP antagonist, as recently demonstrated also for $Ca_v1.3\alpha1$ (Koschak et al., 2001). We could exploit a "natural mutation," an amino acid exchange from tyrosine to phenylalanine in position 1414 (Fig. 8), of the DHP-binding domain to investigate the role of this residue for agonist action. In $Ca_v1.1\alpha1$ (data not shown), $Ca_v1.2\alpha1$, and $Ca_v1.3\alpha1$, a tyrosine is found in this position (Tyr1463; $\alpha1$C-a numbering) (Striessnig et al., 1998). Mutation of this residue to phenylalanine was found to decrease DHP antagonist-binding affinity at least in $Ca_v1.1\alpha1$ (Peterson et al., 1996). We show that the tyrosine to phenylalanine exchange in $Ca_v1.4\alpha1$ does not cause a major change in DHP antagonist sensitivity, as compared with $Ca_v1.3\alpha1$. The role of this tyrosine for DHP agonist sensitivity has not been investigated thus far. Because we found a robust stimulation of $Ca_v1.4\alpha1$-mediated currents by BayK 8644, we can clearly demonstrate that the tyrosine hydroxyl is not required for BayK 8644 stimulation of LTCCs.

Functional implications

Our data provide a first answer to the important question whether $Ca_v1.4\alpha1$ LTCCs can contribute to the L-type currents in retinal photoreceptors and bipolar cells, which are tightly coupled to neurosecretion. In photoreceptors (Wilkinson and Barnes, 1996; Taylor and Morgans, 1998; Kourennyi and Barnes, 2000; Stella et al., 2002) and bipolar cells (von Gersdorff and Matthews, 1996; Protti and Llano, 1998) of different species, DHP-sensitive I_{Ca} was found to posses properties not typically found for L-type currents in cardiac myocytes or neurons. These were described as faster activation, slower inactivation, negative activation thresholds, and intermediate DHP sensitivity. Such properties were described previously both in the current study and by others (for review, see Lipscombe, 2002) for $Ca_v1.3\alpha1$. $Ca_v1.3\alpha1$ is expressed in photoreceptor terminals in the outer plexiform layer (OPL) and, most likely, also bipolar cells synapses in the inner plexiform layer (IPL) (Morgans et al., 1998; Taylor and Morgans, 1998; Morgans, 1999). Therefore, these channels could account for the retinal $I_{Ca,L}$ in these cells. However, we can now demonstrate that $Ca_v1.4\alpha1$ can also mediate currents with similar properties. Because $Ca_v1.4\alpha1$ is also expressed in the synapses of the OPL and IPL (Firth et al., 2001; Morgans, 2001; Morgans et al., 2001; Ball et al., 2002; Berntson et al., 2003), it may

also participate in the formation of photoreceptor and bipolar cell $I_{Ca,L}$ (Berntson et al., 2003). In humans, $Ca_v1.4\alpha1$ mutations cause iCSNB2. Most of these mutations result in truncated subunits and should cause a complete loss of function. The most promising animal model to directly quantitate the contribution of $Ca_v1.4\alpha1$ to retinal $I_{Ca,L}$ are $Ca_v1.4\alpha1$-deficient mice. In these animals, one should be able to correlate visual defects with the relative contribution of $Ca_v1.4\alpha1$ to retinal $I_{Ca,L}$. $Ca_v1.3\alpha1$-deficient mice do not seem to represent such a useful model because they do not exhibit electroretinogram changes (Platzer et al., 2000) (M.W. Seeliger, E. Schmid, J. Platzer, and J. Striessnig, unpublished observations).

On the basis of their biophysical characteristics and intermediate DHP sensitivity, $Ca_v1.3\alpha1$ and $Ca_v1.4\alpha1$ might be classified as a functional LTCC subgroup. Because of its lower activation threshold, $Ca_v1.3\alpha1$ has indeed been shown to serve in an essential role for cardiac pacemaking in the sinoatrial node, which cannot be substituted by $Ca_v1.2\alpha1$ expressed in the same cells (Zhang et al., 2002; Mangoni et al., 2003). Faster activation, lower activation thresholds, and slower inactivation make $Ca_v1.3\alpha1$ and $Ca_v1.4\alpha1$ also suited for certain neuronal functions. First, they can support neurotransmitter release from nonspiking neurons and sensory cells such as photoreceptors ($Ca_v1.3\alpha1$ and $Ca_v1.4\alpha1$) and cochlear inner hair cells ($Ca_v1.3\alpha1$). In the latter, >90% of the current is carried by $Ca_v1.3\alpha1$ (Platzer et al., 2000). In the darkness, photoreceptors are continuously depolarized by cGMP-gated channels to approximately −30 to −40 mV. During illumination, they hyperpolarize by approximately −20 to −30 mV (Witkovsky et al., 1997). To rapidly adjust tonic release to changes in illumination (i.e., changes in membrane potential), $I_{Ca,L}$ should be rapidly gated, activated over a relatively negative voltage range, and slowly inactivated at depolarized potentials. These criteria are fulfilled by $Ca_v1.3\alpha1$ and $Ca_v1.4\alpha1$ but not $Ca_v1.2\alpha1$. Second, sustained $I_{Ca,L}$, activating at negative voltages, are suitable to support plateau potentials in neurons elicited, for instance, by weak depolarizations to voltages just above the resting potential of a neuron. For example, such plateau potentials occur in motoneurons (Carlin et al., 2000; Alaburda et al., 2002) and second order pain neurons (Morisset and Nagy, 2000), in which they modulate motoneuron responses and pain processing, respectively. Such current components are believed to be mediated by $Ca_v1.3\alpha1$ (Carlin et al., 2000; Alaburda et al., 2002), but systematic analysis of $Ca_v1.4\alpha1$ expression (e.g., in motoneurons) has not yet been performed. Similarly, in bipolar cell nerve terminals, such low voltage-activated L-type Ca^{2+} currents also seem to account for the interesting finding that specific retinal bipolar cells, which are generally considered nonspiking cells, can respond to light-induced tonic depolarization by photoreceptors with Ca^{2+} action potentials and regenerative responses from a plateau potential (Burrone and Lagnado, 1997; Protti et al., 2000), mechanisms that are suitable to amplify small photoreceptor signals. Additional studies will have to determine the inactivation kinetics of $Ca_v1.3\alpha1$ and $Ca_v1.4\alpha1$ on even longer time scales than those shown here. Note that in mouse cochlea inner hair cells, $Ca_v1.3\alpha1$-mediated currents inactivate to a much smaller extent than after heterologous expression (Zidanic and Fuchs, 1995; Kollmar et al., 1997; Platzer et al., 2000). It will be important to reveal the molecular substrate of this difference, which may not be only attributable to alternative splicing of $\alpha1$ subunits (Koschak et al., 2001; Safa et al., 2001; Xu and Lipscombe, 2001).

Our work demonstrates for the first time that $Ca_v1.4\alpha1$ subunits form functional LTCCs that can contribute to such currents. Therefore, this study paves the way for the analysis of $Ca_v1.4\alpha1$ mutations responsible for iCSNB2. A detailed genotype–phenotype analysis of this disease will now be possible.

References

Alaburda A, Perrier JF, Hounsgaard J (2002) Mechanisms causing plateau potentials in spinal motoneurones. Adv Exp Med Biol 508:219–226.

Ball SL, Powers PA, Shin HS, Morgans CW, Peachey NS, Gregg RG (2002) Role of the beta(2) subunit of voltage-dependent calcium channels in the retinal outer plexiform layer. Invest Ophthalmol Vis Sci 43:1595–1603.

Bech-Hansen NT, Naylor MJ, Maybaum TA, Pearce WG, Koop B, Fishman GA, Mets M, Musarella MA, Boycott KM (1998) Loss-of-function mutations in a calcium-channel alpha1-subunit gene in Xp11.23 cause incomplete X-linked congenital stationary night blindness. Nat Genet 19:264–267.

Berntson A, Taylor WR, Morgans CW (2003) Molecular identity, synaptic localization, and physiology of calcium channels in retinal bipolar cells. J Neurosci Res 71:146–151.

Bourinet E, Charnet P, Tomlinson WJ, Stea A, Snutch TP, Nargeot J (1994) Voltage-dependent facilitation of a neuronal α_{1C} L-type calcium channel. EMBO J 13:5032–5039.

Bourinet E, Soong TW, Stea A, Snutch TP (1996) Determinants of the G protein-dependent opioid modulation of neuronal calcium channels. Proc Natl Acad Sci USA 431:470–472.

Boycott KM, Maybaum TA, Naylor MJ, Weleber RG, Robitaille J, Miyake Y, Bergen AA, Pierpont ME, Pearce WG, Bech-Hansen NT (2001) A summary of 20 CACNA1F mutations identified in 36 families with incomplete X-linked congenital stationary night blindness, and characterization of splice variants. Hum Genet 108:91–97.

Budde T, Meuth S, Pape HC (2002) Calcium-dependent inactivation of neuronal calcium channels. Nat Rev Neurosci 3:873–883.

Burrone J, Lagnado L (1997) Electrical resonance and Ca^{2+} influx in the synaptic terminal of depolarizing bipolar cells from the goldfish retina. J Physiol (Lond) 505:571–584.

Canti C, Page KM, Stephens GJ, Dolphin AC (1999) Identification of residues in the N terminus of alpha1B critical for inhibition of the voltage-dependent calcium channel by $G_{\beta\gamma}$. J Neurosci 19:6855–6864.

Carlin KP, Jones KE, Jiang Z, Jordan LM, Brownstone RM (2000) Dendritic L-type calcium currents in mouse spinal motoneurons: implications for bistability. Eur J Neurosci 12:1635–1646.

Castellano A, Wei X, Birnbaumer L, Perez-Reyes E (1993) Cloning and expression of a third calcium channel beta subunit. J Biol Chem 268:3450–3455.

Catterall WA (2000) Structure and regulation of voltage-gated calcium channels. Annu Rev Cell Dev Biol 16:521–555.

Dai S, Klugbauer N, Zong X, Seisenberger C, Hofmann F (1999) The role of subunit composition on prepulse facilitation of the cardiac L-type calcium channel. FEBS Lett 442:70–74.

de Leon M, Wang Y, Jones L, Perez-Reyes E, Wei X, Soong TW, Snutch TP, Yue DT (1995) Essential Ca^{2+}-binding motif for Ca^{2+}-sensitive inactivation of L-type Ca^{2+} channels. Science 270:1502–1506.

Ellis SB, Williams ME, Ways NR, Brenner R, Sharp AH, Leung AT, Campbell KP, McKenna E, Koch WJ, Hui A, Schwartz A, Harpold MM (1988) Sequence and expression of mRNAs encoding the alpha1 and alpha2 subunits of a DHP-sensitive calcium channel. Science 241:1661–1664.

Firth SI, Morgan IG, Boelen MK, Morgans CW (2001) Localization of voltage-sensitive L-type calcium channels in the chicken retina. Clin Experiment Ophthalmol 29:183–187.

Grabner M, Dirksen RT, Beam KG (1998) Tagging with green fluorescent protein reveals a distinct subcellular distribution of L-type and non-L-type Ca^{2+} channels expressed in dysgenic myotubes. Proc Natl Acad Sci USA 95:1903–1908.

Graef IA, Mermelstein PG, Stankunas K, Neilson JR, Deisseroth K, Tsien RW, Crabtree GR (1999) L-type calcium channels and GSK-3 regulate the activity of NF-ATc4 in hippocampal neurons. Nature 401:703–708.

Herlitze S, Hockerman GH, Scheuer T, Catterall WA (1997) Molecular determinant of inactivation and G protein modulation in the intracellular loop connecting domains I and II of the calcium channel alpha 1A subunit. Proc Natl Acad Sci USA 94:1512–1516.

Huber I, Wappl E, Herzog A, Mitterdorfer J, Glossmann H, Langer T, Striessnig J (2000) Conserved Ca^{2+} antagonist binding properties and putative folding structure of a recombinant high affinity dihydropyridine binding domain. Biochem J 347:829–836.

Kamp TJ, Hu H, Marban E (2000) Voltage-dependent facilitation of cardiac L-type Ca channels expressed in HEK-293 cells requires beta-subunit. Am J Physiol Heart Circ Physiol 278:H126–H136.

Kollmar R, Fak J, Montgomery LG, Hudspeth AJ (1997) Hair cell-specific splicing of mRNA for the alpha1D subunit of voltage-gated Ca^{2+} channels in the chicken's cochlea. Proc Natl Acad Sci USA 94:14889–14893.

Koschak A, Reimer D, Huber I, Grabner M, Glossmann H, Engel J, Striessnig J (2001) alpha 1D (Cav1.3) subunits can form l-type Ca^{2+} channels activating at negative voltages. J Biol Chem 276:22100–22106.

Kourennyi DE, Barnes S (2000) Depolarization-induced calcium channel facilitation in rod photoreceptors is independent of G proteins and phosphorylation. J Neurophysiol 84:133–138.

Liang H, DeMaria CD, Erickson MG, Mori M, Alseikhan BA, Yue DT (2003) Toward a unified mechanism for calcium regulation of the calcium channel family. Biophys J 84:405.

Lipscombe D (2002) L-type calcium channels: highs and new lows. Circ Res 90:933–935.

Mangoni ME, Couette B, Bourinet E, Platzer J, Reimer D, Striessnig J, Nargeot J (2003) Functional role of L-type Cav1.3 calcium channels in cardiac pacemaker activity. Proc Natl Acad Sci USA 100:5543–5548.

Meza U, Adams B (1998) G-Protein-dependent facilitation of neuronal alpha1A, alpha1B, and alpha1E Ca^{2+} channels. J Neurosci 18:5240–5252.

Mikami A, Imoto K, Tanabe T, Niidome T, Mori Y, Takeshima H, Narumiya S, Numa S (1989) Primary structure and functional expression of the cardiac dihydropyridine-sensitive calcium channel. Nature 340:230–233.

Morgans CW (1999) Calcium channel heterogeneity among cone photoreceptors in the tree shrew retina. Eur J Neurosci 11:2989–2993.

Morgans CW (2001) Localization of the alpha(1F) calcium channel subunit in the rat retina. Invest Ophthalmol Vis Sci 42:2414–2418.

Morgans CW, El Far O, Berntson A, Wassle H, Taylor WR (1998) Calcium extrusion from mammalian photoreceptor terminals. J Neurosci 18:2467–2474.

Morgans CW, Gaughwin P, Maleszka R (2001) Expression of the alpha1F calcium channel subunit by photoreceptors in the rat retina. Mol Vis 7:202–209.

Morisset V, Nagy F (2000) Plateau potential-dependent windup of the response to primary afferent stimuli in rat dorsal horn neurons. Eur J Neurosci 12:3087–3095.

Mouton J, Feltz A, Maulet Y (2001) Interactions of calmodulin with two peptides derived from the c-terminal cytoplasmic domain of the Ca(v)1.2 Ca^{2+} channel provide evidence for a molecular switch involved in Ca^{2+}-induced inactivation. J Biol Chem 276:22359–22367.

Murakami M, Nakagawasai O, Fujii S, Kameyama K, Murakami S, Hozumi S, Esashi A, Taniguchi R, Yanagisawa T, Tan-no K, Tadano T, Kitamura K, Kisara K (2001) Antinociceptive action of amlodipine blocking N-type Ca^{2+} channels at the primary afferent neurons in mice. Eur J Pharmacol 419:175–181.

Naylor MJ, Rancourt DE, Bech-Hansen NT (2000) Isolation and characterization of a calcium channel gene, cacna1f, the murine orthologue of the gene for incomplete X-linked congenital stationary night blindness. Genomics 66:324–327.

Pan ZH (2000) Differential expression of high- and two types of low-voltage-activated calcium currents in rod and cone bipolar cells of the rat retina. J Neurophysiol 83:513–527.

Pate P, Mochca-Morales J, Wu Y, Zhang JZ, Rodney GG, Serysheva II, Williams BY, Anderson ME, Hamilton SL (2000) Determinants for calmodulin binding on voltage-dependent Ca^{2+} channels. J Biol Chem 275:39786–39792.

Perez-Reyes E, Castellano A, Kim HS, Bertrand P, Baggstrom E, Lacerda AE, Wei X, Birnbaumer L (1992) Cloning and expression of a cardiac/brain β subunit of the L-type calcium channel. J Biol Chem 267:1792–1797.

Peterson BZ, Tanada TN, Catterall WA (1996) Molecular determinants of high affinity dihydropyridine binding in L-type calcium channels. J Biol Chem 271:5293–5296.

Peterson BZ, Lee JS, Mulle JG, Wang Y, de Leon M, Yue DT (2000) Critical determinants of Ca^{2+}-dependent inactivation within an EF-hand motif of L-type Ca($^{2+}$) channels. Biophys J 78:1906–1920.

Pitt GS, Zuhlke RD, Hudmon A, Schulman H, Reuter H, Tsien RW (2001) Molecular basis of calmodulin tethering and Ca^{2+}-dependent inactivation of L-type Ca^{2+} channels. J Biol Chem 276:30794–30802.

Platzer J, Engel J, Schrott-Fischer A, Stephan K, Bova S, Chen H, Zheng H, Striessnig J (2000) Congenital deafness and sinoatrial node dysfunction in mice lacking class D L-type calcium channels. Cell 102:89–97.

Protti DA, Llano I (1998) Calcium currents and calcium signaling in rod bipolar cells of rat retinal slices. J Neurosci 18:3715–3724.

Protti DA, Flores-Herr N, von Gersdorff H (2000) Light evokes Ca^{2+} spikes in the axon terminal of a retinal bipolar cell. Neuron 25:215–227.

Qin N, Olcese R, Bransby M, Lin T, Birnbaumer L (1999) Ca^{2+}-induced inhibition of the cardiac Ca^{2+} channel depends on calmodulin. Proc Natl Acad Sci USA 96:2435–2438.

Romanin C, Gamsjaeger R, Kahr H, Schaufler D, Carlson O, Abernethy DR, Soldatov NM (2000) Ca^{2+} sensors of L-type Ca^{2+} channel. FEBS Lett 487:301–306.

Safa P, Boulter J, Hales TG (2001) Functional properties of Cav1.3 (alpha1D) L-type Ca^{2+} channel splice variants expressed by rat brain and neuroendocrine GH3 cells. J Biol Chem 276:38727–28737.

Safayhi H, Haase H, Kramer U, Bihlmayer A, Roenfeldt M, Ammon HP, Froschmayr M, Cassidy TN, Morano I, Ahlijanian M, Striessnig J (1997) L-type calcium channels in insulin-secreting cells: biochemical characterization and phosphorylation in RINm5F cells. Mol Endocrinol 11:619–629.

Scholze A, Plant TD, Dolphin AC, Nurnberg B (2001) Functional expression and characterization of a voltage-gated CaV1.3 (alpha1D) calcium channel subunit from an insulin-secreting cell line. Mol Endocrinol 15:1211–1221.

Soldatov NM, Zuhlke RD, Bouron A, Reuter H (1997) Molecular structures involved in L-type calcium channel inactivation. Role of the carboxyl-terminal region encoded by exons 40–42 in alpha1C subunit in the kinetics and Ca^{2+} dependence of inactivation. J Biol Chem 272:3560–3566.

Stella Jr SL, Bryson EJ, Thoreson WB (2002) A2 adenosine receptors inhibit calcium influx through L-type calcium channels in rod photoreceptors of the salamander retina. J Neurophysiol 87:351–360.

Striessnig J, Grabner M, Mitterdorfer J, Hering S, Sinnegger MJ, Glossmann H (1998) Structural basis of drug binding to L calcium channels. Trends Pharmacol Sci 19:108–115.

Strom TM, Nyakatura G, Apfelstedt-Sylla E, Hellebrand H, Lorenz B, Weber BH, Wutz K, Gutwillinger N, Ruther K, Drescher B, Sauer C, Zrenner E, Meitinger T, Rosenthal A, Meindl A (1998) An L-type calcium-channel gene mutated in incomplete X-linked congenital stationary night blindness. Nat Genet 19:260–263.

Taylor WR, Morgans C (1998) Localization and properties of voltage-gated calcium channels in cone photoreceptors of Tupaia belangeri. Vis Neurosci 15:541–552.

von Gersdorff H, Matthews G (1996) Calcium-dependent inactivation of calcium current in synaptic terminals of retinal bipolar neurons. J Neurosci 16:115–122.

Wappl E, Koschak A, Poteser M, Sinnegger MJ, Walter D, Eberhart A, Groschner K, Glossmann H, Kraus RL, Grabner M, Striessnig J (2002) Functional consequences of P/Q-type Ca^{2+} channel Cav2.1 missense mutations associated with episodic ataxia type 2 and progressive ataxia. J Biol Chem 277:6960–6966.

Welling A, Ludwig A, Zimmer S, Klugbauer N, Flockerzi V, Hofmann F (1997) Alternatively spliced IS6 segments of the alpha 1C gene determine the tissue-specific dihydropyridine sensitivity of cardiac and vascular smooth muscle L-type Ca^{2+} channels. Circ Res 81:526–532.

Wilkinson MF, Barnes S (1996) The dihydropyridine-sensitive calcium channel subtype in cone photoreceptors. J Gen Physiol 107:621–630.

Witkovsky P, Schmitz Y, Akopian A, Krizaj D, Tranchina D (1997) Gain of rod to horizontal cell synaptic transfer: relation to glutamate release and a dihydropyridine-sensitive calcium current. J Neurosci 17:7297–7306.

Xu W, Lipscombe D (2001) Neuronal $Ca_v1.3$alpha(1) L-type channels activate at relatively hyperpolarized membrane potentials and are incompletely inhibited by dihydropyridines. J Neurosci 21:5944–5951.

Zhang JF, Ellinor PT, Aldrich RW, Tsien RW (1996) Multiple structural elements in voltage-dependent calcium channels support their inhibition by G proteins. Neuron 17:991–1003.

Zhang Z, Xu Y, Song H, Rodriguez J, Tuteja D, Namkung Y, Shin HS, Chiamvimonvat N (2002) Functional roles of $Ca_v1.3$ (alpha1D) calcium channel in sinoatrial nodes: insight gained using gene-targeted null mutant mice. Circ Res 90:981–987.

Zidanic M, Fuchs PA (1995) Kinetic analysis of barium currents in chick cochlear hair cells. Biophys J 68:1323–1336.

Zuhlke RD, Pitt GS, Deisseroth K, Tsien RW, Reuter H (1999) Calmodulin supports both inactivation and facilitation of L-type calcium channels. Nature 399:159–162.